



TITLE:

Insertable inductively coupled volumetric coils for MR microscopy in a human 7T MR system

AUTHOR(S):

Okada, Tomohisa; Handa, Shinya; Ding, Bill; Urayama, Shin-ichi; Fujimoto, Koji; Shima, Atsushi; Yoshii, Daisuke; ... Onoe, Hirotaka; Isa, Tadashi; Petropoulos, Labros

CITATION:

Okada, Tomohisa ...[et al]. Insertable inductively coupled volumetric coils for MR microscopy in a human 7T MR system. *Magnetic Resonance in Medicine* 2022, 87(3): 1613-1620

ISSUE DATE:

2022-03










URL:

<http://hdl.handle.net/2433/276219>

RIGHT:

This is an open access article under the terms of the Creative Commons Attribution Non-Commercial-NoDerivs License, which permits use and distribution in any medium, provided the original work is properly cited, the use is non-commercial and no modifications or adaptations are made.; © 2021 The Authors. *Magnetic Resonance in Medicine* published by Wiley Periodicals LLC on behalf of International Society for Magnetic Resonance in Medicine.

Insertable inductively coupled volumetric coils for MR microscopy in a human 7T MR system

Tomohisa Okada¹  | Shinya Handa²  | Bill Ding² | Shin-ichi Urayama¹ |
Koji Fujimoto¹  | Atsushi Shima¹  | Daisuke Yoshii³  | Takashi Ayaki³  |
Nobukatsu Sawamoto⁴  | Ryosuke Takahashi³  | Hirotaka Onoe¹ |
Tadashi Isa¹  | Labros Petropoulos²

¹Human Brain Research Center, Graduate School of Medicine, Kyoto University, Kyoto, Japan

²Quality Electrodynamics, Mayfield Village, Ohio, USA

³Department of Neurology, Graduate School of Medicine, Kyoto University, Kyoto, Japan

⁴Department of Human Health Sciences, Graduate School of Medicine, Kyoto University, Kyoto, Japan

Correspondence

Tomohisa Okada, Human Brain
Research Center, Graduate School of
Medicine, Kyoto University, 54 Shogoin
Kawaharacho, Sakyoku, Kyoto 606-8507
Japan.
Email: tomokada@kuhp.kyoto-u.ac.jp

Funding information

This research was supported by the
Japan Agency for Medical Research and
Development (AMED project numbers:
21dm0307003h0004 and 20dm0207093)

Purpose: To demonstrate the capability of insertable inductively coupled volumetric coils for MR microscopy in a human 7T MR system.

Methods: Insertable inductively coupled volume coils with diameters of 26 and 64 mm (D26 and D64 coils) targeted for monkey and mouse brain specimen sizes were designed and fabricated. These coils were placed inside the imaging volume of a transmit/receive knee coil without wired connections to the main system. Signal-to-noise ratio (SNR) evaluations were conducted with and without the insertable coils, and the g-factor maps of parallel imaging (PI) were also calculated for the D64 coil. Brain specimens were imaged using 3D T₂*-weighted images with spatial resolution of isotropic 50 and 160 μm using D26 and D64 coils, respectively.

Results: Relative average (SD) SNRs compared with knee coil alone were 12.54 (0.30) and 2.37 (0.05) at the center for the D26 and D64 coils, respectively. The mean g-factors of PI with the D64 coil for the factor of 2 were less than 1.1 in the left-right and anterior-posterior directions, and around 1.5 in the superior-inferior direction or when the PI factor of 3 was used. Acceleration in two directions showed lower g-factors but suffered from intrinsic low SNR. Representative T₂*-weighted images of the specimen showed structural details.

Conclusion: Inductively coupled small diameter coils insertable to the knee coil demonstrated high SNR and modest PI capability. The concept was successfully used to visualize fine structures of the brain specimen. The insertable coils are easy to handle and enable MR microscopy in a human whole-body 7T MRI system.

Tomohisa Okada and Shinya Handa contributed equally to this work.

This is an open access article under the terms of the Creative Commons Attribution-NonCommercial-NoDerivs License, which permits use and distribution in any medium, provided the original work is properly cited, the use is non-commercial and no modifications or adaptations are made.

© 2021 The Authors. *Magnetic Resonance in Medicine* published by Wiley Periodicals LLC on behalf of International Society for Magnetic Resonance in Medicine.

KEYWORDS

connection-free, human 7 Tesla, inductive coupling, knee coil, microimaging, unplugged insertable coil

1 | INTRODUCTION

The human 7T MR scanner is increasing its availability and enables high-resolution and/or special contrast imaging using modern pulse sequences. It can be used not only as a clinical diagnostic tool but also as a research tool for *ex vivo* imaging. It is a common practice to validate human image findings *in vivo* on specimen or animal models. A dedicated animal MR system is usually used to scan small samples to obtain high spatial resolution. However, some pulse sequences are provided only to a human scanner, and some samples are too large for a small-bore scanner. It is highly desirable that we can image specimens using the same human MR scanner. A high signal-to-noise ratio (SNR) for a small object can be attained by matching the sizes of specimen and coil. Building dedicated multi-channel phased-array coils for small objects¹⁻³ is a usual choice, but fabrication of such multi-channel phased-array coils and their integration into scanner comes with complexity.

In general, current human MR systems are furnished with large-sized multi-element human coils, and they should be leveraged. To improve filling factor and SNR, a small size coil with close proximity to samples is required. One way to achieve such a high SNR on a small sample without disturbing the human scanner electronics is to use a small-size coil that is tightly couple to the sample to create high local sensitivity and can be inserted and used in human coils without wiring. Furthermore, if the small insertable coil is coupled with a multi-channel phased-array design of the primary coil, parallel imaging can be achieved that leads to faster scan time.⁴⁻⁶

Here, we fabricated connection-free (“unplugged”) insertable volume coils targeted for representative brain specimen of the monkey and mouse that were inductively coupled with a commercial knee array coil without wiring and demonstrated the capability of this combined system to improve SNR and image resolution for small samples using a human 7T-MR system.

2 | METHODS

2.1 | Design and setup

An investigational whole-body human 7T scanner (MAGNETOM 7T, Siemens Healthineers, Erlangen, Germany) and a single-channel transmit and 28-channel

receive knee coil (Quality Electrodynamics, Mayfield Village, OH, USA)⁷ were selected as the baseline system. The inner diameter of the knee coil is approximately 15 cm and the total 28 receive elements are arranged in three rows of 10, 8, and 10 elements as shown in Supporting Information Figure S1A, which is available online. Representative specimen would be the brains of the monkey and mouse, which would be around 60 and 20 mm, respectively, in the largest diameter. Many of the human brain specimen lie within this range; thus, we fabricated two unplugged insertable volume coils designed to fit into the knee coil with inner diameters of 26 and 64 mm (D26 and D64 coils, see Supporting Information Figure S1B,C).

The coil frames of the D26 and D64 coils were designed in Solidworks (Dassault Systemes, France) and 3D printed from polycarbonate (Fortus 400mc, Stratasys, US). The D26 coil was a four-turn solenoid coil with two passive decoupling circuits (total coil length: 5 cm; coil inner and outer diameters: 2.6 and 3.5 cm) and made of 3 mm width tinned copper strips. The D64 coil was a quadrature saddle coil with capacitive decoupling network and four passive decoupling circuits (total coil length: 8 cm; coil inner and outer diameters: 6.4 and 7.3 cm) and made of 10 mm width tinned copper strips. For a small coil as D26, the solenoid design is one of the best for high SNR at small diameter (less than 40 mm), but it is not so for a coil with a larger diameter as in D64 due to large inductance and radiation loss and the saddle coil design was adopted. See Figure 1 for configuration and Figure 2 for equivalent schematic diagrams and parts description.

These coils are placed inside of the knee coil and designed to inductively couple to the knee coil, thus no wiring to the main system is required. While the insertable volume coils were coupled to the knee coil in receive phase, the formers were decoupled to the latter by the built-in passive decoupling circuits in transmit phase, and no transmit B1 field enhancement or distortion was observed. When the knee coil was in the receive state, the insertable coils were inductively coupled to the knee receive array coils and generated a uniformly enhanced B1 field distribution within the localized resonator. Each knee receive array element is decoupled by a low noise and low input impedance preamplifier.⁷

2.2 | SNR and g-factor evaluation

The SNR evaluation was conducted using a 3D gradient-echo imaging (field of view [FOV] = 77 mm, repetition

FIGURE 1 Views of insertable coil arrangements. (A) A D26 coil view with a trimmer capacitor and the other from the opposite side. (B) Two orthogonal views of the D64 coil. These limited views are provided, because only copper elements exist in the views orthogonal to the presented ones of the D26 coil, and the opposite views of the D64 coil are the same

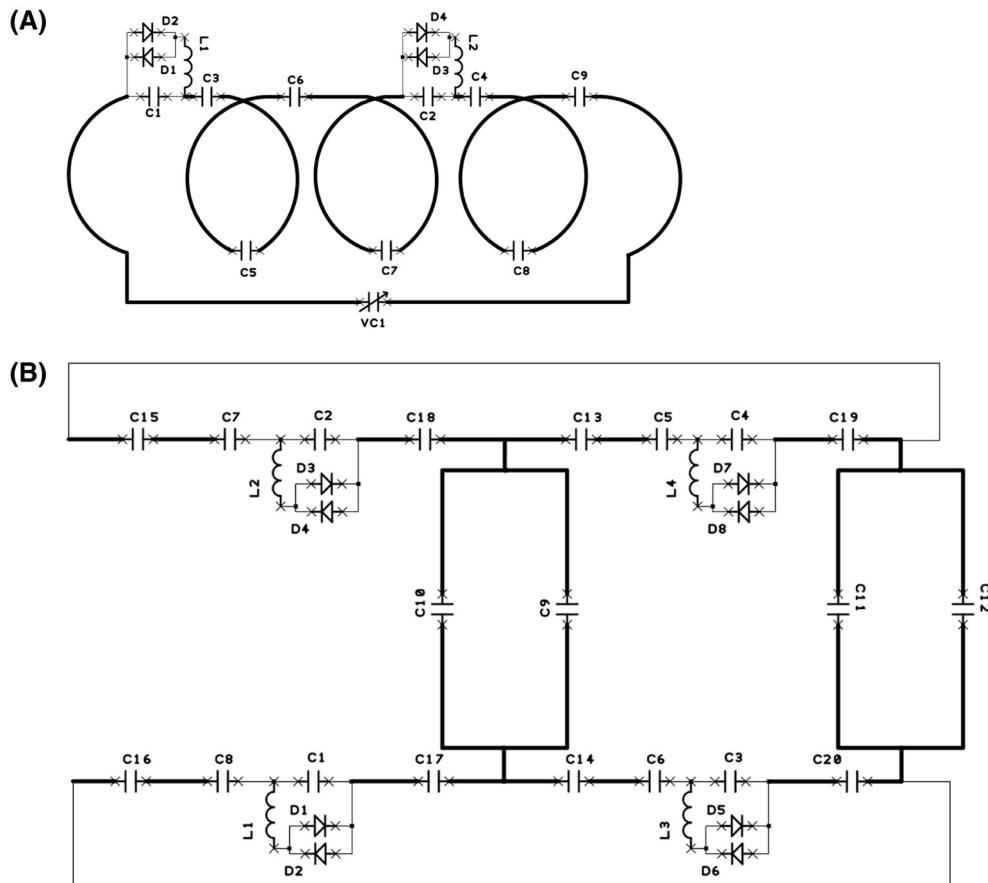
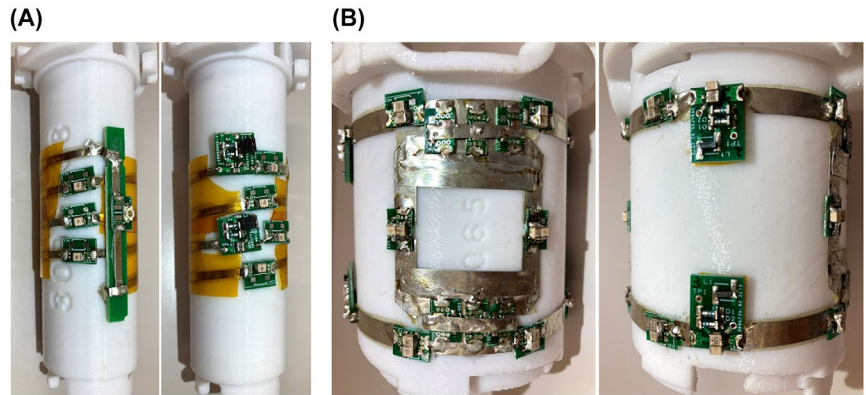


FIGURE 2 Equivalent circuit diagrams of D26 (A) and D64 (B) coils. The D26 coil is a four-turn solenoid coil (parts: C1, C2 = 9 pF, fixed capacitors [R15S series, Johanson Technology Inc., Camarillo, CA, US]; C3, C4 = 8.2 pF, C5–C9 = 4.3 pF, fixed capacitors [ATC100B series, American Technical Ceramics, Huntington Station, NY, US]; L1, L2 = 22 nH [Midi Spring Air Core Inductors, Coilcraft Inc., Cary, IL, US]; VC1: 2–6pF Trimmer Capacitor [JZ060HV, Knowles Voltronics, Cazenovia, NY, US]) and the D64 coil is a quadrature saddle coil (parts: C1–C4 = 14.2pF, C5–C8 = 11.1 pF, C9–C12 = 19 pF, C13–C20 = 14 pF, fixed capacitors [ATC100B series, American Technical Ceramics, Huntington Station, NY, US]; L1–L4 = 9.85 nH [Micro Spring Air Core Inductors, Coilcraft Inc., Cary, IL, US]). All diodes used in the D26 and D64 coils are fast MRI protection diode (UMX9989SM, Microsemi, Irvine, CA, US)

time/echo time [TR/TE] = 50/11 ms, bandwidth= 40 Hz/pixel, resolution = 300 μm isotropic) of phantom bottles filled with saline solution using the knee coil with and without two insertable coils. The flip angles were 14 and 0 degrees for image signal and noise measurements,

respectively. The SNR maps of D26 and D64 coil images were calculated in relation to images acquired using the knee coil only. As a reference, a wired eight-channel phased-array receive coil with the inner and outer diameters of 55 and 60 mm (D55 wired coil, Takashima

Seisakusho, Tokyo, Japan. See Supporting Information Figure S2), which is the only existing onsite coil with a similar diameter, was also evaluated for relative SNR. Transmission was conducted using a birdcage coil with a diameter of 29 cm (Takashima Seisakusho, Tokyo, Japan). Using the same phantom, relative SNR of the D64 coil was also measured and compared.

To analyze g-factor maps of parallel imaging, fully encoded datasets were measured using phantom bottles filled with saline doped with a gadolinium-based MR contrast agent (Gadodiamide; GE Healthcare, Japan) so that its T1 relaxation time was approximately 200 ms. The scans were conducted for a single slice of 2-mm thick in three orthogonal directions (axial, coronal, and sagittal to the bore axis) with and without the insert coils. The parameters were as follows: TR/TE = 100/10 ms, bandwidth = 80 Hz/pixel, and resolution = 300 μm isotropic. The FOVs were 120 and 80 mm for the D26 and D64 coils, respectively. The flip angles were 40 and 0 degrees for signal and noise measurements, respectively. Four averages were used for scans with the insert coils and 32 (maximum) for those with the knee coil. The fully encoded dataset acquired using the D64 coil was used to calculate g-factor maps of parallel imaging (this was not conducted for the D26 coil because the coil sensitivity was highly localized).

In the SNR comparison, SNR scaled reconstruction based on the Kellman method⁸ was implemented in Python 3.8 (Python software foundation, Delaware, USA) on a 24-core dual 3.6 GHz Intel Xeon Gold 6256 PC with 192 GB DRAM. The Siemens Healthineers standard reconstruction methods were also used for the reconstruction. The g-factor calculations were performed using the pygrappa library (<https://github.com/mckib2/pygrappa>). In the home-built python scripts, the twixtools was used for importing a scanner raw-data (<https://github.com/mrphysics-bonn/twixtools>), and the imported *k*-space data was fed into NumPy array (<https://numpy.org/>) for the actual reconstruction pipelines accelerated in left-right (LR), anterior-posterior (AP), and superior-inferior (SI) directions. Regions-of-interest (ROIs) analysis was conducted on the relative SNR maps at their center by placing circular ROIs with diameter of 30 pixels using ImageJ 1.50i (<https://imagej.nih.gov/ij/>). In the comparison of D55 and D64 coils, circular ROIs of 10 pixels were placed at the peripheral area in addition to the central ROIs.

2.3 | Ex vivo specimen scans

The scans of both human and the other animal samples were approved by the institutional review board (R1472-5). Ex vivo brain specimens were prepared in proton-free susceptibility-matching fluid (Fluorinert FC-43, 3M Corp.,

MN, USA) and imaged using a 3D gradient-echo sequence for T₂*-weighted images. For the D26 coil, a formalin-fixed frontal lobe tissue of a 77-y-old neuronal intranuclear inclusion disease (NIID) patient with many amyloid plaques showing frequent CERAD neuritic plaque score⁹ was scanned in isotropic 50 μm resolution with two sets of parameters: TR/TE/FA = 200 ms/23 ms/24° and 100 ms/23 ms/18°. The scan times (hours:minutes) were 2:30 and 1:15, respectively. The FOV and bandwidth were the same (20 mm and 30 Hz/pixel).

For the D64 coil, a macaque brain prepared with the gadolinium-based MR contrast agent¹⁰ was scanned in isotropic 160 μm resolution (FOV = 72 mm, TR/TE = 200/20 ms, bandwidth = 30 Hz/pixel). Scan times were 4:02, 2:21, 1:48, and 1:06 with acceleration factors of 1, 2, 3, and 2 × 2, respectively. The macaque brain was placed in a position similar to that of the human brain in the supine position.

2.4 | Histopathology

For comparison with the corresponding T₂*-weighted images, the brain specimen of the NIID patient with many amyloid plaques was stained for amyloid- β and iron. The specimen was embedded in paraffin and serially cut into a 6- μm -thick section and a 20- μm -thick section. The 6- μm -thick section was used for amyloid- β immunohistochemistry. After deparaffinization, this section was pretreated with formic acid to enhance immunoreactivity. We performed immunostaining using mouse monoclonal antibodies against amyloid- β (clone 6E10, 803002; BioLegend, San Diego, CA, USA; 1:1000) as a primary antibody and a Simple Stain MAX-PO Kit (424152; Histofine, Nichirei, Tokyo, Japan) as a secondary antibody. Reaction products were visualized with 3,3'-diaminobenzidine (DAB) using a DAB Substrate Kit (SK-4100; Vector Laboratories, Burlingame, CA, USA), followed by counterstaining cell nuclei with hematoxylin. The 20- μm -thick section was used for histochemical iron detection by the Perls method supplemented by intensification with DAB/CoCl₂.^{11,12} After dewaxing/rehydration, this section was incubated for 30 min in equal volumes of freshly prepared 2% potassium ferrocyanide and 2% hydrochloric acid (final 1% combined concentration for each), washed, and incubated for 10 min in a solution containing DAB/CoCl₂ made using a DAB Substrate Kit. The reaction was stopped by washing.

3 | RESULTS

The average (SD) relative SNR values were 12.54 (0.30) and 2.37 (0.05) for D26 and D64 coils, respectively, at the

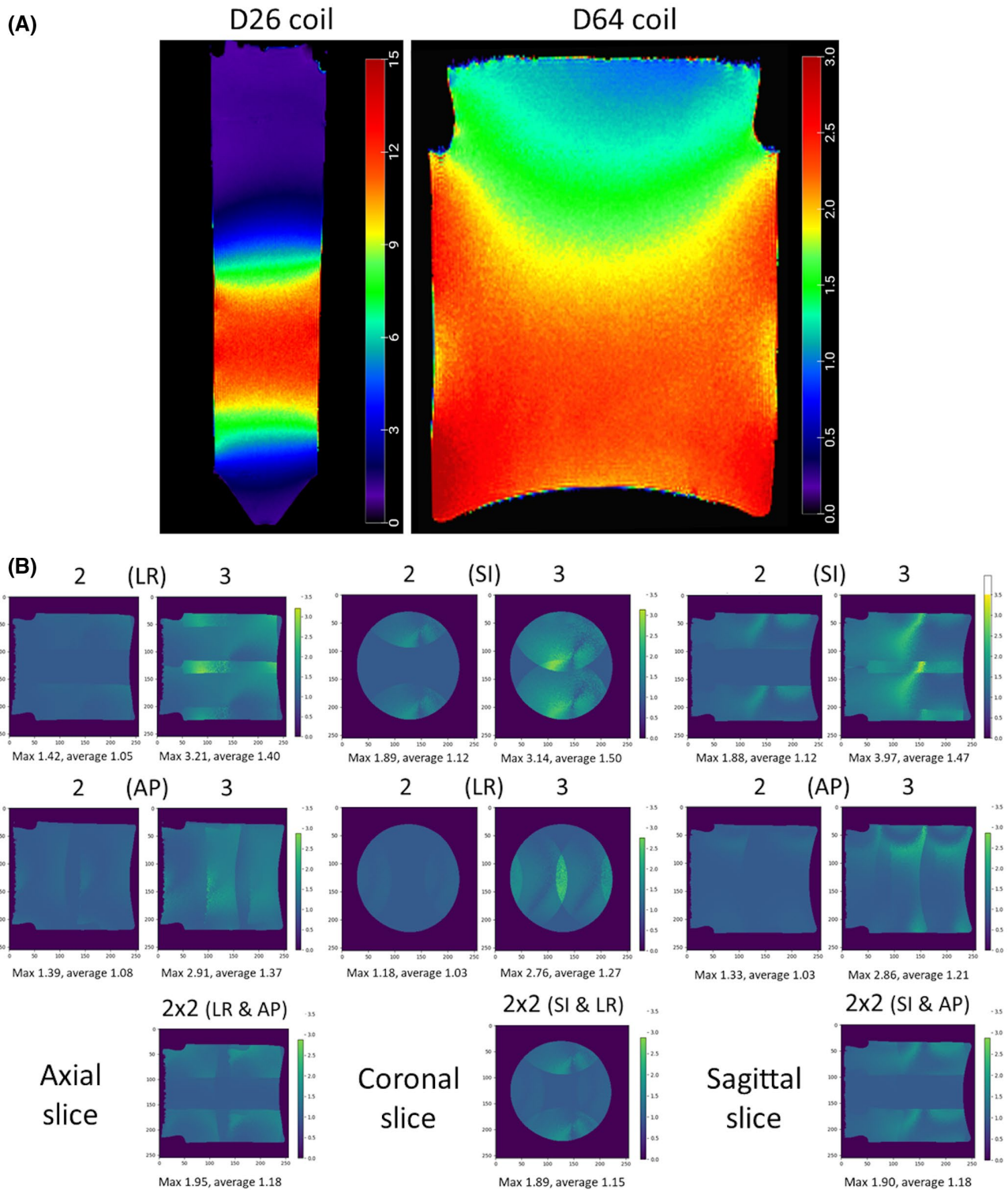


FIGURE 3 (A) Relative SNR maps. SNR gains versus knee coil alone were around 12-fold and 2.5-fold at the center for D26 and D64 coils, respectively. (B) Parallel imaging factors and g-factor maps. The parallel imaging factors are presented above the g-factor maps. The directions of acceleration are also presented in parenthesis (LR: left-right; AP: anterior-posterior; and SI: superior-inferior directions). Relatively small g-factors were observed with the acceleration factor of 2, especially in LR and AP directions compared with SI direction. The parallel factor of 3 showed maximum g-factor of around 3 or higher. The acceleration factor of 2 in two directions (2×2) had maximum g-factors of less than 2

center when the matched phantoms were scanned. In the comparison between D55 and D64 coils measuring the same phantom, the values were 2.8 (0.1) and 15.3 (2.6) for the D55 coil and 6.5 (0.1) and 7.9 (0.3) for the D64 coil at the center and periphery, respectively. Relative SNR maps for D26 and D64 insertable coils inductively coupled with the knee coil are shown in Figure 3A. Those for comparison between D55 and D64 coils are presented in Supporting Information Figure S3.

The average increase in g-factors of parallel imaging with the D64 coil for the acceleration factor of 2 were less than 10% in the LR and AP directions, but it was 12% in the SI direction. For the parallel imaging with acceleration factor of 3, the average and maximum g-factors were around 1.5 and 3–4, respectively, and use might be limited. However, acceleration by the factors of 2×2 in two directions, showed lower g-factors than accelerating by 3 in one direction (Figure 3B).

Representative images of the specimens are shown in Figures 4 (D26) and 5 (D64). In the brain specimen of the NIID patient with many amyloid plaques, many small dark dots were observed located at the cerebral cortex (Figure 4). These are considered to be amyloid plaques with iron deposition. The small plaques could be visualized on T_2^* -weighted images because of the blooming effect caused by their high susceptibility in addition to high spatial resolution.^{13–15} In the macaque brain, fine laminar structures of the hippocampus and lateral geniculate nucleus were observed when no acceleration was applied (Figure 5). Structural details of the cerebellar folia, brain stem, basal ganglia and thalamus are also depicted. A

comparable image was obtained when the acceleration factor of 2 was applied, but noise was more conspicuous when the factor was increased to 3 or 2×2 .

4 | DISCUSSION

High-resolution imaging of specimens on a human 7T-MR scanner is feasible in a practical and simple manner, when the unplugged insertable volume coils were used. The proposed insertable coils were used with the knee coil without modification of the coil interface, and their setup is very easy. Scan parameters need to be optimized depending on the sample size and target contrast. The representative scan was T_2^* -weighted imaging, because a low bandwidth was required to retain SNR from very small voxels and the TE became long. However, the TE can be set at a smaller value, and new sequences created for human scans would be used for the specimen and potentially for small animals in vivo.

When the unwired insertable D64 coil was compared with the wired eight-channel D55 coil for relative SNR, the D64 coil had 2.3 and 0.5 times of relative SNR at the center and periphery, respectively. As Supporting Information Figure S3 shows, SNR distribution is relatively homogeneous for the combination of D64 and knee coils, whereas it is heterogeneous for the D55 coil. The homogeneous SNR distribution of the D64 coil can be more advantageous than the highly localized high SNR of the D55 coil, because the specimen is frequently nearly the size of the coil diameter. The homogeneous relative SNR distribution

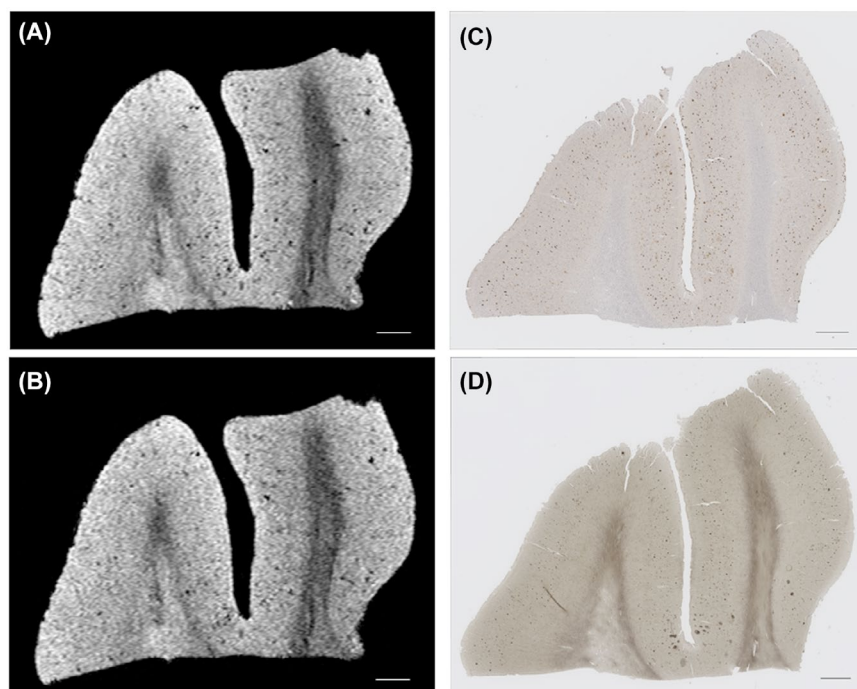
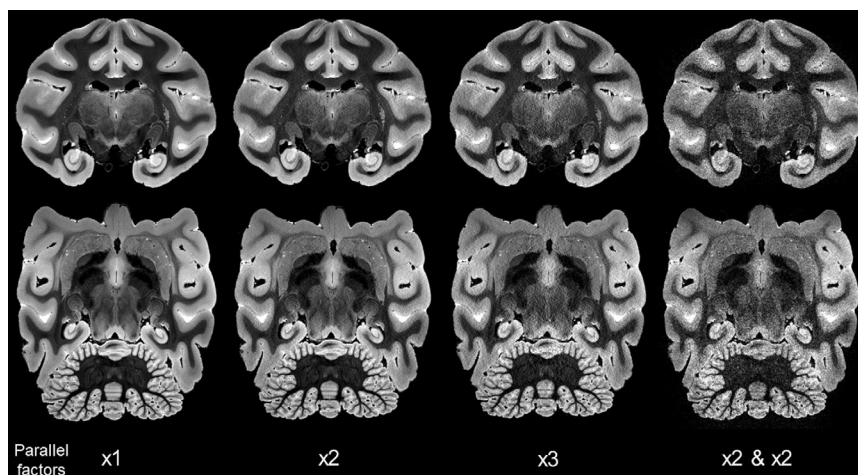


FIGURE 4 Brain specimen of a neuronal intranuclear inclusion disease patient with many amyloid plaques. On the left are T_2^* -weighted images of a brain specimen acquired using the D26 coil with isotropic $50 \mu\text{m}$ resolution in TR/TE/FA (ms/ms/degrees) of 200/24/24 (A) and 100/24/18 (B). Numerous tiny low-signal dots are observed. Similar contrast was attained when TR was cut in half. (C) Amyloid- β immunohistochemistry shows numerous amyloid plaques. (D) Iron staining shows iron deposition at the amyloid plaques. This iron deposition was considered to be the cause of the low-signal dots. (A-D) Scale bars: 1 mm

FIGURE 5 A whole brain imaging of a macaque specimen acquired using the D64 solenoid coil in isotropic $160\ \mu\text{m}$ resolution with the acceleration factors of 1, 2, 3, and 2×2 (from left to right). No foldover artifact was observed. With the acceleration factor of 2, the image is comparable to that without acceleration, but noise was slightly higher in 3 and 2×2 conditions, especially at the image center



of the D64 coil is considered as the result from the insertable volume resonator design and inductive coupling to the knee coil with larger diameter.

For the primary coil, we had two choices for the 7T MR system: a 32-channel head coil and the 28-channel knee coil. The former is dome shaped and larger in diameter. Because of the probable longer distance and inhomogeneity of inductive coupling, the head coil was not used, although no test was conducted.

A long scan time is required for high-resolution imaging. For specimens, it may not be a problem, because scans can be conducted at night. When the scanner availability is limited, parallel imaging can be used for the D64 coil. For the D26 coil, parallel imaging resulted in relatively large g -factor due to its small size and little difference in coil sensitivity of the knee coil elements. However, the D26 coil has a high SNR, and TR can be reduced for a faster scan.

For an animal scan in vivo, a shorter scan time is preferable, and parallel imaging can be used for the D64 coil. The acceleration factor can be up to 3 or 2×2 , but the acceleration factor of 3 should be limited to the LR and AP directions. The g -factor becomes higher in the SI direction due to the coil array layout of the knee coil. The knee array coil has up to 10 elements in the one row to accommodate acceleration of LR and AP direction, whereas those in the SI direction have only three rows as shown in Supporting Information Figure S1A.

Compared to parallel imaging in one direction, versus two directions, i.e., 2×2 shows little directional preference, because acceleration in both LR and AP directions share the same elements. Such directional non-preference for parallel imaging in two directions allows flexible set up of the specimen. In addition to a shorter scan time, parallel imaging capability would be used to reduce image distortion in, e.g., diffusion scanning. However, as noted in actual images presented in Figure 5, increasing the acceleration factors and reducing the scan time result

in intrinsic reduction of SNR in addition to the g -factor penalty.

The long axis of the insertable coils needs to be placed orthogonal to the B_0 direction, which is the direction of the knee coil diameter (approximately 15 cm). Even though the current configuration of insertable volume coils has a limited flexibility of sample size and orientation, this limitation can be ameliorated with different configurations of inductively coupled resonators such as birdcage coils or dielectric resonators.¹⁶ Such a coil can provide horizontal bore access for animal scans in vivo under anesthesia with high SNR.

This study was conducted using a human 7T system. A similar setup can be configured for 3T and 1.5T. At these static magnetic fields, high-resolution imaging requires more averaging, but the capability of using the same scan sequences developed for humans to specimens and small animals will facilitate imaging research.

5 | CONCLUSIONS

Inductively coupled and connection-free small diameter coils that can be easily inserted into the knee coil could successfully visualize fine structures of specimen. They are easy to handle and enable MR microscopy using the same whole-body 7T-MRI system that is used for human subjects. The inductively coupled small-diameter volume coils are expected to perform well even at 3T and 1.5T, although such validation is yet to be conducted.

ACKNOWLEDGMENT

This research was supported by the Japan Agency for Medical Research and Development, (AMED project numbers: 21dm0307003h0004 and 20dm0207093). The authors are grateful to Profs. Takashi Hanakawa and Toshiya Murai for their help with this study.

CONFLICT OF INTEREST

S.H., B.D., and L.P. are employees of Quality Electrodynamics. T.O. is supported by a research grant from Siemens Healthcare KK, Japan (not related to this study).

ORCID

Tomohisa Okada  <https://orcid.org/0000-0003-2312-5677>

Shinya Handa  <https://orcid.org/0000-0003-3286-5132>

Koji Fujimoto  <https://orcid.org/0000-0003-1209-7949>

Atsushi Shima  <https://orcid.org/0000-0002-3068-4621>

Daisuke Yoshii  <https://orcid.org/0000-0001-9817-3337>

Takashi Ayaki  <https://orcid.org/0000-0003-0189-5910>

Nobukatsu Sawamoto  <https://orcid.org/0000-0001-8695-0223>

Ryosuke Takahashi  <https://orcid.org/0000-0002-1407-9640>

Tadashi Isa  <https://orcid.org/0000-0001-5652-4688>

REFERENCES

- Zhang B, Sodickson DK, Cloos MA. A high-impedance detector-array glove for magnetic resonance imaging of the hand. *Nat Biomed Eng.* 2018;2:570-577.
- Zhang B, Brown R, Cloos M, Lattanzi R, Sodickson D, Wiggins G. Size-adaptable, “Trellis” structure for tailored MRI coil arrays. *Magn Reson Med.* 2019;81:3406-3415.
- Lakshmanan K, Cloos M, Brown R, Lattanzi R, Sodickson DK, Wiggins GC. The “Loopole” antenna: a hybrid coil combining loop and electric dipole properties for ultra-high-field MRI. *Concepts Magn Reson Part B Magn Reson Eng.* 2020;2020:8886543.
- Sodickson DK, Manning WJ. Simultaneous acquisition of spatial harmonics (SMASH): fast imaging with radiofrequency coil arrays. *Magn Reson Med.* 1997;38:591-603.
- Jakob PM, Griswold MA, Edelman RR, Sodickson DK. AUTO-SMASH: a self-calibrating technique for SMASH imaging. Simultaneous acquisition of spatial harmonics. *MAGMA.* 1998;7:42-54.
- Pruessmann KP, Weiger M, Scheidegger MB, Boesiger P. SENSE: sensitivity encoding for fast MRI. *Magn Reson Med.* 1999;42:952-962.
- Finnerty M, Yang X, Zheng T, et al. A 7-tesla high density transmit with 28-channel receive-only array knee coil. *Proc Intl Soc Mag Reson Med.* 2010;18:642.
- Kellman P, McVeigh ER. Image reconstruction in SNR units: a general method for SNR measurement†. *Magn Reson Med.* 2005;54:1439-1447.
- Mirra SS, Heyman A, McKeel D, et al. The consortium to establish a registry for Alzheimer’s disease (CERAD): part II. Standardization of the neuropathologic assessment of Alzheimer’s disease. *Neurology.* 1991;41:479.
- Zhang X, Bearer EL, Perles-Barbacaru AT, Jacobs RE. Increased anatomical detail by in vitro MR microscopy with a modified Golgi impregnation method. *Magn Reson Med.* 2010;63:1391-1397.
- Meguro R, Asano Y, Odagiri S, Li C, Iwatsuki H, Shoumura K. Nonheme-iron histochemistry for light and electron microscopy: a historical, theoretical and technical review. *Arch Histol Cytol.* 2007;70:1-19.
- van Duijn S, Nabuurs RJA, van Duinen SG, Natté R. Comparison of histological techniques to visualize iron in paraffin-embedded brain tissue of patients with Alzheimer’s disease. *J Histochem Cytochem.* 2013;61:785-792.
- Jack CR, Garwood M, Wengenack TM, et al. In vivo visualization of Alzheimer’s amyloid plaques by magnetic resonance imaging in transgenic mice without a contrast agent. *Magn Reson Med.* 2004;52:1263-1271.
- House MJ, St. Pierre TG, Kowdley KV, et al. Correlation of proton transverse relaxation rates (R2) with iron concentrations in postmortem brain tissue from Alzheimer’s disease patients. *Magn Reson Med.* 2007;57:172-180.
- Chamberlain R, Reyes D, Curran GL, et al. Comparison of amyloid plaque contrast generated by T2-weighted, -weighted, and susceptibility-weighted imaging methods in transgenic mouse models of Alzheimer’s disease. *Magn Reson Med.* 2009;61:1158-1164.
- Ruytenberg T, Webb AG. Design of a dielectric resonator receive array at 7 Tesla using detunable ceramic resonators. *J Magn Reson.* 2017;284:94-98.

SUPPORTING INFORMATION

Additional supporting information may be found in the online version of the article at the publisher’s website.

FIGURE S1 (A) Coil arrangements of the 1-channel transmit and 28-channel receive knee coil. Placement of insertable coils with diameters of (B) 26 mm (D26) and (C) 64 mm (D64) inside of the knee coil with (top) and without (bottom) the upper knee coil element. No wiring for the D26 and D64 coils is required. Ant: anterior, P: posterior, L: left, R: right, S: superior and I: inferior

FIGURE S2 The wired coil. (A) A view of the wired phased-array 8-channel receive coil with inner diameter of 55 mm (D55 coil). (B) An equivalent schematic diagram of a coil element is illustrated by the authors, because the circuit diagram of the D55 coil was not available from the manufacturer. The D55 coil consists of the same 8 elements

FIGURE S3 SNR maps of the (A) D55 wired and (B) D64 insertable coils relative to the phantom image SNR acquired using the 28-channel knee coil

How to cite this article: Okada T, Handa S, Ding B, et al. Insertable inductively coupled volumetric coils for MR microscopy in a human 7T MR system. *Magn Reson Med.* 2022;87:1613–1620. doi:[10.1002/mrm.29062](https://doi.org/10.1002/mrm.29062)

WOULD YOU LIKE TO POST AN INFORMAL COMMENT ABOUT THIS PAPER, OR ASK THE AUTHORS A QUESTION ABOUT IT?

If so, please visit <https://mrm.ismrm.org/> and register for our Magn Reson Med Discourse site (registration is free).

The screenshot displays the Magn Reson Med Discourse website. At the top, there is a search bar and a 'New Topic' button. Below the navigation bar, the 'MRM Papers' category is highlighted, showing a list of 164 papers. The 'Latest' section on the right lists three featured papers:

- [April 2022] Reproducible Research Insights with Jakob Assländer (0 comments, 16d)
- MRM Highlights Magazine - Volume 7 (0 comments, 16d)
- [April 2022] Q&A with Jakob Assländer and Daniel Sodickson (0 comments, 16d)

Magn Reson Med is currently listing the top 8 downloaded papers from each issue (including Editor's Picks) for comments and questions on the Discourse web site.

However, we are happy to list this or any other papers (please email mrm@ismrm.org to request the posting of any other papers.)

We encourage informal comment and discussion about Magn Reson Med papers on this site. Please note, however, that a formal errata from the authors should still be submitted in the usual way via our Manuscript Central online submission system.